Compatibility-Modulated Stability Thresholds in Nonlinear Dynamical Systems

Geometric Contraction and Network Synchronization

Ori Manzur[a,*]

[a] reBORN Research Initiative, Israel

ARTICLE INFO

Keywords:
Nonlinear dynamical systems
Stability thresholds
Synchronization
Fast–slow systems
Invariant manifolds

ABSTRACT

Alignment and synchronization in interacting dynamical systems are typically characterized by threshold conditions on coupling strength, which is often treated as a prescribed or freely state-dependent quantity. In contrast, the structural origin of how interaction strength may increase endogenously within a fixed interaction topology remains less explicitly constrained.

We introduce a compatibility-based framework for coupled nonlinear fast–slow systems in which effective coupling strength is modulated through a monotone incompatibility–integration cascade. Each subsystem carries a non-negative incompatibility functional whose decay induces derived quantities—including coherence amplitude, correlation measures, and an integration scale—that enter multiplicatively into the effective coupling while preserving the baseline interaction graph.

Under standard regularity, boundedness, and timescale separation assumptions, this cascade induces monotone non-decrease of effective coupling along trajectories in an admissible regime. We show that once the resulting interaction strength exceeds a finite critical threshold in a neighborhood of the compatibility manifold, the transverse dynamics become locally contractive, yielding exponential convergence toward compatibility states and decay of cross-system mismatch.

The framework thereby recovers a classical threshold mechanism of nonlinear dynamics—stabilization through dominance of interaction strength over intrinsic divergence—while providing a structural explanation for how such thresholds may be crossed through endogenous modulation of effective coupling without altering interaction topology.

1. Introduction

Coordinated behavior in coupled nonlinear dynamical systems—including synchronization, alignment, and collective pattern formation—typically emerges when interaction strength exceeds a critical stability threshold. Classical nonlinear dynamics provides rigorous frameworks for analyzing such phenomena, including invariant manifold theory, singular perturbation methods for fast–slow systems, and contraction-type stability arguments [7, 4]. In these formulations, however, interaction amplitudes are usually treated either as fixed parameters or as generic state-dependent functions, without structural constraints linking internal improvements in subsystem compatibility to systematic modulation of interaction strength under a fixed interaction graph. This limits the ability of existing formulations to explain how systems may cross classical stability thresholds through internally generated changes in interaction strength.

This leaves open a structural question: how can interaction strength increase endogenously in a way that is both dynamically consistent and topologically constrained, and sufficient to drive systems across classical stability thresholds? In particular, existing formulations do not isolate mechanisms through which reductions in internal incompatibility can accumulate into increased effective coupling without introducing new interaction channels or prescribing explicit gain dynamics.

Connection to classical models. This question appears implicitly in several well-studied settings in nonlinear dynamics. For example, in phase oscillator systems, synchronization occurs when coupling strength exceeds a detuning-dependent threshold, while in networked systems stability is governed by Laplacian-weighted interaction strength. In these classical formulations, however, the coupling amplitude is externally prescribed or treated as a free parameter. The

*Corresponding author.
manzurori4@gmail.com (O. Manzur)

present framework provides a structural mechanism by which such thresholds can be crossed endogenously, recovering the same threshold conditions while explaining how the required interaction strength may arise internally.

The present work identifies such a mechanism within a constrained class of classical nonlinear dynamical systems. Each subsystem is equipped with a nonnegative incompatibility functional F_i that vanishes on an internal compatibility set. Along trajectories within an admissible regime, F_i is assumed non-increasing. This monotone decay is mapped through a chain of monotone C^1 transformations

$$F_i \longmapsto \alpha_i \longmapsto (\xi_i, \tau_i) \longmapsto \Gamma_i, \tag{1}$$

where Γ_i defines an *integration scale*. This incompatibility–integration cascade provides a structured pathway by which local reductions in incompatibility accumulate into larger scales of internal coherence within interacting subsystems.

Effective coupling is then restricted to the factorized form

$$\kappa_{ij}^{\mathrm{eff}} = \kappa_{ij}\, Q(\Gamma_i)\, R(\Gamma_j), \tag{2}$$

where $\kappa_{ij} \geq 0$ are baseline interaction coefficients and Q, R are non-decreasing functions. A central architectural constraint is *no-channel creation*,

$$\kappa_{ij} = 0 \implies \kappa_{ij}^{\mathrm{eff}} = 0, \tag{3}$$

so that the interaction graph remains invariant and all state dependence enters through derived scale variables.

This structure defines a strict subclass of generic C^1 state-dependent coupling laws. While general coupling functions may depend arbitrarily on the full system state and effectively alter graph structure, the factorized form (2) enforces multiplicative separability and constrains gain modulation to node-level integration variables. Combined with monotone incompatibility decay, this implies that effective coupling strengths are monotone non-decreasing along trajectories within the admissible regime.

Within this architecture, compatibility improvement acquires a direct dynamical consequence: it systematically increases effective interaction strength and can drive the system across classical stabilization thresholds without modifying the underlying interaction topology. In particular, this provides a mechanism through which classical threshold-governed behaviors can emerge from internally generated changes in effective coupling strength.

Main result (informal). Within a forward-invariant compact regime W, and under the scalar effective-gain specialization used in the explicit contraction theorem, the mismatch dynamics transverse to the compatibility manifold $\mathcal{C} := \{E = 0\}$ admit a Jacobian decomposition of the form

$$J_\perp(z, \Gamma) = D(z) - g_{\mathrm{eff}}(\Gamma)\, C(z),$$

where D represents intrinsic transverse curvature generated by uncoupled subsystem dynamics and C represents curvature induced by coupling interactions. If the symmetric part of C is uniformly positive along $W \cap \mathcal{C}$, then there exists a finite threshold g_{crit} such that whenever $g_{\mathrm{eff}}(\Gamma) \geq g_{\mathrm{crit}} + \mu$ for some $\mu > 0$ in a neighborhood of $W \cap \mathcal{C}$, the transverse distance to the compatibility manifold contracts and trajectories converge exponentially toward $\mathcal{C}$. Because the cascade (1) induces monotone non-decrease of the effective gain under this specialization, stabilization can be achieved through endogenous gain modulation within the architecture, thereby recovering a classical threshold mechanism through internally generated interaction strength.

Throughout the analysis we restrict attention to a forward-invariant compact regime W, ensuring the uniform bounds required for the transverse stability arguments. All contraction results are derived for the fast subsystem obtained by freezing the slow variables ($\varepsilon = 0$), so that the slow variables act as parameters on the contraction timescale.

Contributions. Within this framework the paper establishes the following structural results:

1. **Constrained endogenous coupling structure.** A factorized integration-modulated coupling class (2) that preserves baseline graph sparsity via the no-channel-creation constraint (3).
2. **Monotone gain evolution.** Under monotone incompatibility decay and monotone cascade mappings, the integration scale Γ_i is non-decreasing along admissible trajectories, implying monotone non-decrease of effective coupling strengths.
3. **Finite transverse contraction threshold.** A curvature-dominance condition yields an explicit finite threshold g_{crit} ensuring uniform transverse contraction toward the compatibility manifold in the fast subsystem.

4. **Scale-consistent stabilization principle.** The same dominance mechanism appears in network synchronization settings, showing that classical threshold conditions can be recovered within a compatibility-modulated coupling architecture across multiple dynamical scales.

Position of the present contribution. The stabilization results derived in Section 4 follow from classical transverse contraction arguments once the gain structure is specified. The contribution of the present work is to identify a constrained structural mechanism within this classical framework through which interaction gains evolve via a monotone incompatibility–integration cascade while preserving the baseline interaction topology. Within this class, improvements in subsystem compatibility systematically increase effective coupling strength and can drive the system across stabilization thresholds without introducing new interaction channels, thereby providing a structural explanation for threshold-governed behavior in classical dynamical systems.

Scope of the contraction theorem. The structural framework introduced above allows heterogeneous pairwise effective couplings of the form

$$\kappa_{ij}^{\mathrm{eff}} = \kappa_{ij} Q(\Gamma_i) R(\Gamma_j).$$

The explicit transverse contraction theorem derived in Section 4 is established for a scalar effective-gain specialization of the projected coupling operator,

$$C(z_c, \Gamma) = g_{\mathrm{eff}}(\Gamma)\, \widetilde{C}(z_c),$$

or equivalently for settings in which a uniform lower bound on stabilizing gain factors can be defined along trajectories in the admissible regime. This specialization provides a tractable setting for explicit analysis while remaining consistent with the broader factorized coupling architecture. A full characterization of when the heterogeneous factorized coupling law admits such a scalar effective-gain reduction remains an open analytical problem.

Organization. Section 2 positions the structural constraints relative to existing work on state-dependent and adaptive coupling, synchronization thresholds, and fast–slow reduction. Section 3 specifies the admissible regime and formal definitions. Section 4 derives the transverse Jacobian decomposition and the curvature-dominance threshold guaranteeing local contraction toward the compatibility manifold, and presents the networked-oscillator illustration. Sections 5–7 discuss implications, limitations, and scope.

2. Background

Nonlinear dynamical systems theory provides the mathematical foundation for analyzing stability, bifurcations, synchronization, and collective behavior in interacting systems [8, 6, 16]. A central theme in this literature is the emergence of coherent dynamics through interaction-induced reshaping of transverse stability, typically analyzed using invariant manifold theory, contraction arguments, and spectral properties of linearized dynamics.

Coupling-induced collective behavior. In many canonical models of synchronization and pattern formation, interaction strength is treated as a fixed parameter multiplying a prescribed coupling function. Examples include the Kuramoto phase oscillator model and its generalizations [11, 14, 15]. In these frameworks, the existence and stability of collective states are governed by threshold relations between intrinsic divergence rates and coupling amplitudes.

More generally, in networked dynamical systems, stability is determined by spectral properties of the coupling operator, such as Laplacian eigenvalues. The master stability framework formalizes this separation of node dynamics and network structure, showing that stability depends on the product of coupling gain and network spectrum [13]. In all such formulations, however, the coupling strength itself is externally specified.

State-dependent and adaptive coupling. To move beyond fixed gains, many models introduce state-dependent or adaptive coupling mechanisms, allowing interaction strength to evolve with system state or through auxiliary dynamics. Examples include activity-dependent coupling, plastic networks, and adaptive synchronization schemes in which coupling gains obey additional differential equations.

While these approaches capture self-organized synchronization and adaptation, they typically allow broad functional freedom in how coupling depends on state. Coupling laws may depend arbitrarily on global system variables, auxiliary parameters, or mismatch measures, and often modify effective interaction structure through cross-terms or additional dynamical variables.

Fast–slow systems and structural modulation. Fast–slow systems provide a natural framework for studying interactions between rapidly evolving states and slowly adapting structural variables [3, 5, 9, 10]. Under timescale separation, invariant slow manifolds persist and reduced dynamics govern long-term behavior. These methods rigorously describe multiscale adaptation and feedback between dynamics and structure.

However, fast–slow theory does not by itself impose structural constraints on how effective coupling strengths depend on internal variables. In particular, it does not restrict how endogenous variables should modulate interaction gains, nor does it prevent modifications of the underlying interaction topology.

Structural gap. Across these frameworks, a common feature emerges: either interaction strength is prescribed, or it is allowed to vary with broad functional freedom. What is not isolated is a constrained mechanism through which interaction strength increases endogenously in a manner that is both monotone and topologically consistent.

In particular, existing formulations do not identify structural conditions under which reductions in internal incompatibility can systematically accumulate into increased effective coupling while preserving the baseline interaction graph and without introducing additional coupling dynamics.

Structural restriction considered here. The present work isolates such a mechanism within a restricted class of state-dependent coupling laws. Each subsystem is endowed with a nonnegative incompatibility functional F_i that measures deviation from an internal compatibility set. Along trajectories within an admissible regime, F_i is assumed non-increasing. This monotone decay is mapped through a fixed cascade of monotone C^1 transformations,

$$F_i \;\longmapsto\; \alpha_i \;\longmapsto\; (\xi_i, \tau_i) \;\longmapsto\; \Gamma_i,$$

where Γ_i defines an integration scale.

Effective coupling is then restricted to the factorized form

$$\kappa_{ij}^{\mathrm{eff}} = \kappa_{ij}\, Q(\Gamma_i)\, R(\Gamma_j),$$

with Q, R non-decreasing and $\kappa_{ij} \geq 0$ baseline couplings. A key constraint is preservation of the interaction graph:

$$\kappa_{ij} = 0 \quad \Longrightarrow \quad \kappa_{ij}^{\mathrm{eff}} = 0.$$

State dependence therefore enters exclusively through derived integration variables, and cannot introduce new interaction channels.

Relation to existing theory. The resulting architecture lies within the general class of state-dependent couplings but forms a strict structural subset characterized by:

1. multiplicative separability of coupling gains,
2. monotone gain evolution driven by incompatibility decay,
3. invariance of the baseline interaction topology.

Within this constrained class, effective coupling strength evolves monotonically along admissible trajectories and can drive the system across classical stabilization thresholds.

Contribution of this work. The contribution of the present paper is to identify and analyze this minimal structural mechanism within classical nonlinear dynamical systems theory. Under the stated constraints, monotone incompatibility decay induces endogenous growth of effective coupling that can cross a finite stabilization threshold without modifying interaction topology or introducing additional coupling dynamics.

The remainder of the paper formalizes this structural class and derives explicit transverse contraction conditions under which trajectories converge toward the compatibility manifold, with observable mismatch decaying as a consequence of geometric stabilization.

3. Formal Framework

3.1. Phase Space and Well-Posedness

Let the fast variables $x_i \in \mathbb{R}^{n_i}$ and slow variables $\lambda_i \in \mathbb{R}^{m_i}$, and define the joint state vector

$$z = (x_1, \lambda_1, x_2, \lambda_2) \in X,$$

with phase space

$$X := \mathbb{R}^{n_1} \times \mathbb{R}^{m_1} \times \mathbb{R}^{n_2} \times \mathbb{R}^{m_2}.$$

Let the dynamics be generated by a C^2 vector field

$$\mathcal{F} : X \to \mathbb{R}^{\dim X}, \qquad \dot{z} = \mathcal{F}(z).$$

The distinction between fast variables x_i and slow variables λ_i reflects the multiscale structure introduced below.

Forward completeness and absorbing set. We assume the flow of $\mathcal{F}$ is forward complete and admits a compact, positively invariant absorbing set $B \subset X$ such that every bounded set enters B in finite time.

Admissible regime. All analysis is restricted to a forward-invariant subset

$$W \subset B,$$

serving as the admissible regime on which all structural assumptions are required to hold uniformly.

Regularity for geometric analysis. We assume that $\mathcal{F}$ and the mismatch map E are C^2 on an open neighborhood of W. This ensures the existence of normal coordinate charts near the compatibility manifold C, bounded variation of the normal projection operator, and first-order expansions with quadratic remainder in the transverse deviation variable η.

3.2. Prototype Fast–Slow Architecture

For $i \in \{1, 2\}$, consider the fast–slow system

$$\begin{aligned} \dot{x}_i &= f_i(x_i, \lambda_i) + h_i(x_i, x_j, \lambda_i, \lambda_j), \\ \dot{\lambda}_i &= \varepsilon\, g_i(x_i, \lambda_i), \qquad 0 < \varepsilon \ll 1. \end{aligned}$$

All vector fields are assumed C^1 on the admissible regime W.
For $\varepsilon = 0$, the slow variables λ_i are frozen and the dynamics reduce to the fast subsystem

$$\dot{x}_i = f_i(x_i, \lambda_i) + h_i(x_i, x_j, \lambda_i, \lambda_j).$$

This singular perturbation structure allows the transverse stability analysis to be carried out on the fast subsystem, with the slow variables acting as parameters on the contraction timescale. Threshold conditions derived in Section 4 are formulated in this reduced setting.

3.3. Internal Incompatibility Functional

For each subsystem, define a smooth incompatibility functional

$$F_i : \mathbb{R}^{n_i} \times \mathbb{R}^{m_i} \to \mathbb{R}_{\geq 0}, \qquad F_i \in C^1,$$

jointly in (x_i, λ_i).
For each fixed parameter value λ_i, define the internal compatibility set

$$\mathcal{M}_i(\lambda_i) := \{x_i : F_i(x_i; \lambda_i) = 0\}.$$

Assume:

1. $F_i \geq 0$,
2. zero is a regular value of $F_i(\cdot; \lambda_i)$,
3. F_i is bounded on W.

Then for each fixed λ_i, the set $\mathcal{M}_i(\lambda_i)$ is an embedded C^1 submanifold of $\mathbb{R}^{n_i}$, representing the internal compatibility structure toward which subsystem dynamics are organized.

3.4. Coherence Amplitude and Correlation Measures

Define the coherence amplitude

$$\alpha_i := A(F_i),$$

where $A : \mathbb{R}_{\geq 0} \to \mathbb{R}_{\geq 0}$ is C^1 and strictly decreasing, $A'(F) < 0$.

Thus decreasing incompatibility corresponds to increasing coherence.

Define correlation measures

$$\xi_i := \Xi(\alpha_i), \qquad \tau_i := T(\alpha_i),$$

where $\Xi, T : \mathbb{R}_{\geq 0} \to \mathbb{R}_{\geq 0}$ are C^1 and strictly increasing:

$$\Xi'(\alpha) > 0, \qquad T'(\alpha) > 0.$$

By boundedness of F_i on W and continuity of the mappings, α_i, ξ_i, and τ_i are bounded on W.

3.5. Integration Scale

Define the integration scale

$$\Gamma_i := \xi_i \tau_i.$$

We write $\Gamma = (\Gamma_1, \Gamma_2)$ for the vector of node-level integration scales. Effective coupling gains are derived from these variables via the factorized law

$$\kappa_{ij}^{\text{eff}} = \kappa_{ij} Q(\Gamma_i) R(\Gamma_j),$$

so expressions such as $g_{\text{eff}}(\Gamma)$ denote scalar gain factors induced by the vector Γ.

Since ξ_i and τ_i are non-negative, continuous, and bounded on W, the integration scale Γ_i is continuous and bounded on W.

Because $A'(F) < 0$, $\Xi'(\alpha) > 0$, and $T'(\alpha) > 0$, the composite map

$$F_i \longmapsto \Gamma_i$$

is monotone non-increasing. Hence any decrease of F_i along a trajectory implies monotone non-decrease of Γ_i.

The resulting incompatibility–integration cascade is summarized in Fig. 1.

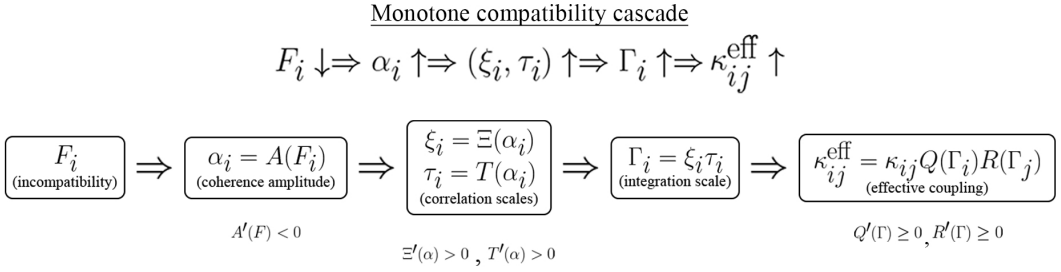

Figure 1: Monotone compatibility cascade. Decreasing incompatibility F_i increases coherence α_i, which increases correlation scales (ξ_i, τ_i), yielding a larger integration scale Γ_i and strengthening the effective coupling κ_{ij}^{eff}.

The variables α_i, ξ_i, and τ_i encode increasing levels of internal coherence, whose accumulation is represented by the integration scale Γ_i. This scale determines the contribution of each subsystem to effective interaction strength.

Relation to cross-system mismatch. The incompatibility measures F_i quantify internal deviation from subsystem-level compatibility, whereas the mismatch function $E(z)$ measures deviation from the compatibility manifold C. The cascade therefore acts indirectly on transverse mismatch dynamics: reductions in F_i increase Γ_i, which increase the effective couplings κ_{ij}^{eff} and may induce contraction toward C without directly constraining $E(z)$.

3.6. Stability Margin and Susceptibility

For each subsystem, consider the intrinsic fast vector field

$$f_i : \mathbb{R}^{n_i} \times \mathbb{R}^{m_i} \to \mathbb{R}^{n_i},$$

assumed C^1 on W.

Spectral bound. Define the maximal intrinsic expansion rate

$$\rho_i(x_i, \lambda_i) := \sup\{\Re(\lambda) : \lambda \in \sigma(D_{x_i} f_i(x_i, \lambda_i))\}.$$

This quantity depends only on the intrinsic Jacobian $D_{x_i} f_i$ and excludes coupling contributions.

Since W is compact and Df_i is continuous, there exists

$$C_{\text{dest}} \geq 0$$

such that

$$\rho_i(x_i, \lambda_i) \leq C_{\text{dest}} \quad \text{for all } (x_i, \lambda_i) \in W.$$

Susceptibility. Let $S : \mathbb{R} \to (0, \infty)$ be C^1 with

$$S'(\mu) \leq 0,$$

and define

$$\chi_i(x_i, \lambda_i) := S\big(\rho_i(x_i, \lambda_i)\big).$$

Thus larger intrinsic expansion rates correspond to smaller susceptibility.

Since ρ_i is bounded on W, χ_i is bounded on W.

3.7. Effective Relational Coupling

Baseline coupling coefficients satisfy

$$\kappa_{ij} \geq 0.$$

Effective couplings are defined by

$$\kappa_{ij}^{\text{eff}} = \kappa_{ij}\, Q(\Gamma_i)\, R(\Gamma_j),$$

where $Q, R : [0, \infty) \to [0, \infty)$ are C^1 non-decreasing functions.

Thus the coupling law is multiplicatively separable in the integration levels of the interacting subsystems.

No-channel creation.

$$\kappa_{ij} = 0 \quad \Longrightarrow \quad \kappa_{ij}^{\text{eff}} = 0.$$

State dependence therefore enters exclusively through the integration scales Γ_i, Γ_j, and the baseline interaction graph is preserved.

Since Γ_i are bounded on W and Q, R are continuous, κ_{ij}^{eff} are continuous and bounded on W.

3.8. Coupled Fast–Slow Dynamics

The coupled fast dynamics are given by

$$\dot{x}_i = f_i(x_i, \lambda_i) - \kappa_{ji}^{\text{eff}}\, \chi_i\, H_{ji}(x_i, x_j),$$

where $H_{ji} : \mathbb{R}^{n_i} \times \mathbb{R}^{n_j} \to \mathbb{R}^{n_i}$ are C^1 interaction maps satisfying $H_{ji}(0, 0) = 0$.

The interaction terms H_{ji} encode cross-system mismatch, while the negative sign represents stabilizing alignment forces that act to reduce this mismatch. The effective coupling κ_{ji}^{eff} modulates the strength of this interaction, and χ_i weights the response by intrinsic susceptibility.

The slow variables evolve according to

$$\dot{\lambda}_i = \varepsilon\, g_i(x_i, \lambda_i), \qquad 0 < \varepsilon \ll 1.$$

Optional coupling-mediated slow adaptation may be included provided that the baseline interaction graph defined by κ_{ij} is preserved.

3.9. Compatibility-Driving Mechanisms

The analysis is restricted to forward-invariant regimes in which the internal incompatibility functionals $F_i(x_i, \lambda_i)$ are non-increasing along trajectories.

Several mechanisms may produce such behavior. Examples include:

(A) Lyapunov-type decay:
$$\dot{F}_i \le -\gamma_i F_i, \qquad \gamma_i > 0,$$
(B) gradient-like slow adaptation of λ_i,
(C) contraction toward the compatibility manifold $\mathcal{C}$ in regimes where effective coupling exceeds the stabilization threshold derived in Section 4.

Any mechanism ensuring monotone decrease of F_i on a forward-invariant subset of W is admissible within this framework.

The present analysis does not derive such mechanisms for the general coupled system, but assumes that the dynamics operate within admissible regimes where incompatibility decay holds. This assumption isolates the structural consequences of the resulting incompatibility–integration cascade.

3.10. Cross-System Mismatch and Compatibility Manifold

Let
$$E : X \to \mathbb{R}^p, \qquad p \ge 1, \qquad E \in C^2,$$
measure cross-system mismatch.

Define the compatibility manifold
$$\mathcal{C} := \{z \in X : E(z) = 0\}.$$

Assume 0 is a regular value of E, i.e.
$$\operatorname{rank} DE(z) = p \quad \text{for all } z \in \mathcal{C}.$$

Then $\mathcal{C}$ is an embedded C^2 submanifold of codimension p.

Mismatch observable versus geometric deviation. We retain the scalar mismatch functional
$$F_{12}(z) := \tfrac{1}{2}\|E(z)\|^2,$$
but transverse stability is analyzed using geometric distance to $\mathcal{C}$ (normal displacement in a tubular neighborhood), rather than $E(z)$ itself as a coordinate.

No a priori stability. No stability of $\mathcal{C}$ is assumed. Section 4 analyzes the transverse dynamics in a neighborhood of $\mathcal{C}$ and derives conditions under which trajectories contract toward the manifold. Exponential decay of F_{12} then follows as a consequence of distance-to-manifold stabilization.

3.11. Composite Observables and Hierarchical Extension

Let
$$Z := \Psi(x_1, x_2), \qquad \Psi : \mathbb{R}^{n_1} \times \mathbb{R}^{n_2} \to \mathbb{R}^k, \qquad \Psi \in C^1,$$
define a composite observable.

On the compatibility manifold $\mathcal{C}$, corresponding composite quantities
$$F_{12}, \quad \alpha_{12}, \quad \xi_{12}, \quad \tau_{12}, \quad \Gamma_{12}$$
may be defined analogously.

Remark 1 (Hierarchical extension)**.** *The compatibility cascade suggests a possible hierarchical extension in which similar mechanisms operate across multiple levels of interacting subsystems. Developing such a multi-scale formulation lies outside the scope of the present work and is left for future study.*

3.12. Admissible Structural Regime

All results are stated relative to a forward-invariant analysis region

$$W \subset B,$$

contained within the absorbing set introduced in Subsection 3.1.

On W the following hold:

1. Df_i is continuous and admits a uniform spectral bound,
$$\sup_{(x_i,\lambda_i)\in W} \rho_i(x_i, \lambda_i) \le C_{\text{dest}} < \infty;$$
2. zero is a regular value of the incompatibility functionals F_i and of the cross-system mismatch map E;
3. the monotonicity assumptions for A, Ξ, T, Q, R, S hold;
4. internal incompatibility F_i is non-increasing along trajectories contained in W (assumed as a standing admissibility condition);
5. the compatibility manifold $C = \{z : E(z) = 0\}$ is invariant under the fast subsystem obtained by freezing the slow variables ($\varepsilon = 0$), i.e.
$$DE(z)\mathcal{F}_{\text{fast}}(z) = 0 \quad \text{for all } z \in C \cap W.$$

All stabilization and threshold results in Section 4 apply to trajectories contained in W.

Relation to adaptive and contraction-based synchronization. The framework is related to adaptive synchronization and contraction-based approaches, but differs in that gain evolution is constrained by a compatibility–integration cascade that preserves the baseline interaction topology.

4. Results

This section analyzes transverse stability of the compatibility manifold

$$C = \{z \in X : E(z) = 0\}.$$

Working in a tubular neighborhood of C, we derive conditions under which the fast subsystem exhibits uniform contraction toward C in directions normal to the manifold. Exponential decay of the mismatch observable $E(z(t))$ then follows from distance-to-manifold stabilization. In this way, the general compatibility–integration architecture is shown to reproduce a familiar threshold principle of nonlinear dynamics: stabilization occurs when effective interaction strength exceeds intrinsic destabilizing curvature or divergence.

All results are stated relative to the admissible regime $W \subset B \subset X$ introduced in Section 3.12. Throughout, we assume:

- All vector fields are C^2 on W.
- Uniform spectral bound: $\rho_i \le C_{\text{dest}}$ on W.
- The monotonicity assumptions for A, Ξ, T, Q, R, S hold on W.
- The analysis is deterministic; stochastic perturbations are not considered.

Unless stated otherwise, contraction results are proved for the fast subsystem ($\varepsilon = 0$), with the slow variables λ_i acting as parameters on the contraction timescale.

Fast–slow interpretation. Throughout this section the slow variables λ_i are treated as frozen parameters ($\varepsilon = 0$), and the results establish transverse contraction for the resulting fast subsystem. Extension of these results to the full fast–slow system with $\varepsilon > 0$ would require additional persistence arguments (e.g., Fenichel-type theory) and is not pursued here.

4.1. Geometry of the Compatibility Manifold and Local Coordinates

Let $E : X \to \mathbb{R}^p$ be the C^2 cross-system mismatch map introduced in Section 3.10. Define the compatibility manifold

$$\mathcal{C} := \{z \in X : E(z) = 0\}.$$

Assume that 0 is a regular value of E. Then $\mathcal{C}$ is an embedded C^2 submanifold of codimension p.

Compatibility invariance condition. As assumed in Subsection 3.12, the compatibility manifold $\mathcal{C}$ is invariant under the fast subsystem obtained by freezing the slow variables ($\varepsilon = 0$). Equivalently,

$$DE(z)\,\mathcal{F}_{\text{fast}}(z) = 0 \quad \text{for all } z \in \mathcal{C} \cap W.$$

This ensures that trajectories starting on $\mathcal{C}$ remain on $\mathcal{C}$ during the fast contraction dynamics analyzed below.

Tangent and normal subspaces (Euclidean metric). For each $z \in \mathcal{C}$,

$$T_z\mathcal{C} = \ker DE(z), \qquad N_z\mathcal{C} := (T_z\mathcal{C})^{\perp} \subset T_zX.$$

Since $DE(z)$ has full rank p on $\mathcal{C}$, the Gram matrix $DE(z)DE(z)^{\top}$ is invertible for all $z \in \mathcal{C}$.

Define the orthogonal projector onto the normal subspace:

$$P_N(z) := DE(z)^{\top}\big(DE(z)DE(z)^{\top}\big)^{-1}DE(z), \qquad z \in \mathcal{C}.$$

Then $P_N(z)$ is symmetric and idempotent, with $\mathrm{Im}(P_N(z)) = N_z\mathcal{C}$.

The local geometry of the compatibility manifold and the associated normal displacement is illustrated schematically in Fig. 2.

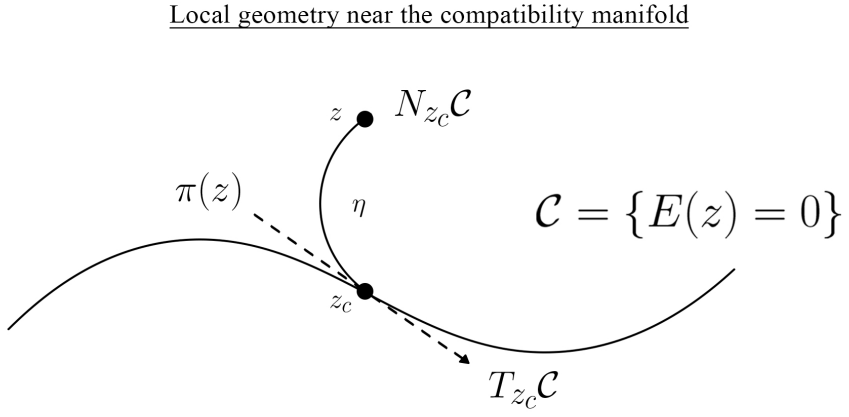

Figure 2: Local geometry near the compatibility manifold $\mathcal{C} = \{E(z) = 0\}$. A nearby state z decomposes into a tangential component along $T_{z_c}\mathcal{C}$ and a transverse displacement η along $N_{z_c}\mathcal{C}$. The projection $\pi(z)$ maps z onto the reference point $z_c \in \mathcal{C}$.

The geometric decomposition illustrated in Fig. 2 underlies the transverse stability analysis developed in the following sections, where deviation from the compatibility manifold is measured by the normal coordinate η.

Local coordinates near the compatibility manifold. Since $E \in C^1$ and 0 is a regular value of E, the implicit function theorem implies that for every $z_c \in \mathcal{C}$ there exists a neighborhood $U_{z_c} \subset X$ and a C^1 coordinate system (y, η) such that

- y parameterizes motion tangent to $\mathcal{C}$,
- $\eta \in \mathbb{R}^p$ (where $p = \mathrm{codim}(\mathcal{C})$) measures deviation transverse to $\mathcal{C}$,
- $\eta = 0$ corresponds to points on $\mathcal{C}$.

In these coordinates the compatibility manifold is locally represented by

$$\mathcal{C} \cap U_{z_c} = \{(y, \eta) : \eta = 0\}.$$

Reference point convention. When analyzing transverse dynamics near $\mathcal{C}$, we denote by $z_c \in \mathcal{C}$ the point corresponding to $\eta = 0$ in the local coordinate representation.

Mismatch observable versus transverse deviation. We retain the observable mismatch

$$e(z) := E(z) \in \mathbb{R}^p,$$

but the transverse analysis below is performed on the deviation variable η defined through the local coordinates above.

Lemma 1 (Local equivalence of mismatch and transverse deviation)**.** *There exist constants $0 < m \le M < \infty$, uniform over $\mathcal{C} \cap \mathcal{W}$, and a neighborhood U_0 of $\mathcal{C} \cap \mathcal{W}$ such that for all $z \in U_0$,*

$$m\,\|\eta(z)\| \;\le\; \|E(z)\| \;\le\; M\,\|\eta(z)\|. \tag{4}$$

Proof. Let (y, η) denote the local coordinates near a point $z_c \in \mathcal{C} \cap \mathcal{W}$ constructed above, with $\eta = 0$ corresponding to z_c. Since $E \in C^1$ and $E(z_c) = 0$, a first-order expansion yields

$$E(z) = DE(z_c)\,\eta + \mathcal{O}(\|\eta\|^2).$$

Because $DE(z_c)$ has full rank and η lies in the normal direction, the restriction $DE(z_c)|_{N_{z_c}\mathcal{C}} : N_{z_c}\mathcal{C} \to \mathbb{R}^p$ is a linear isomorphism. Hence there exist constants $m(z_c), M(z_c) > 0$ such that

$$m(z_c)\|\eta\| \le \|DE(z_c)\eta\| \le M(z_c)\|\eta\|.$$

By compactness of $\mathcal{C} \cap \mathcal{W}$ and continuity of DE, these bounds can be chosen uniformly on $\mathcal{C} \cap \mathcal{W}$. Shrinking the neighborhood absorbs the quadratic remainder, yielding (4). □

4.2. Normal Variational Dynamics and Projected Jacobian Decomposition

We analyze stability *transverse to* $\mathcal{C}$ using the local coordinates (y, η) introduced in Section 4.1, where η measures deviation from the compatibility manifold.

Normal variational equation. Let $z_c(t) \in \mathcal{C} \cap \mathcal{W}$ be a trajectory of the system restricted to $\mathcal{C}$ (an "on-manifold" reference trajectory). Let $z(t)$ be a nearby trajectory in a neighborhood of $\mathcal{C}$ and represent it in local coordinates $(y(t), \eta(t))$.

By C^1 regularity of $\mathcal{F}$, the dynamics admit a first-order Taylor expansion near the reference trajectory $z_c(t)$. In local coordinates (y, η) the transverse deviation therefore satisfies

$$\dot{\eta} = \Big(J_\perp\big(z_c(t), \Gamma(t)\big) + G(z_c(t))\Big)\eta + \mathcal{O}(\|\eta\|^2), \tag{5}$$

where $J_\perp(z_c, \Gamma)$ is the projected Jacobian of the fast vector field and $G(z_c)$ is a geometry operator arising from the variation of the normal projection $P_N(z)$ along trajectories on the manifold.

Because $\mathcal{C} \cap \mathcal{W}$ is compact and both E and $\mathcal{F}$ are C^1, there exists a constant $C_G \ge 0$ such that

$$\|G(z_c)\| \le C_G \quad \text{for all } z_c \in \mathcal{C} \cap \mathcal{W}.$$

Projected normal Jacobian. The transverse Jacobian operator is defined by

$$J_\perp(z_c,\Gamma) := P_N(z_c)\, D_z\mathcal{F}_{\text{fast}}(z_c,\Gamma)\big|_{N_{z_c}\mathcal{C}}, \qquad z_c \in \mathcal{C}\cap W. \tag{6}$$

The restriction in (6) means that $J_\perp$ acts on normal vectors $\eta \in N_{z_c}\mathcal{C}$ and returns vectors in $N_{z_c}\mathcal{C}$.

Projected intrinsic/coupling decomposition. Write the fast subsystem vector field as the difference between intrinsic dynamics and coupling-induced alignment dynamics,

$$\mathcal{F}_{\text{fast}}(z,\Gamma) = \mathcal{F}_{\text{int}}(z) - \mathcal{F}_{\text{cpl}}(z,\Gamma),$$

where $\mathcal{F}_{\text{cpl}}$ collects stabilizing alignment interactions (see Section 3.8).

Define the projected normal Jacobians along $\mathcal{C}\cap W$ by

$$D(z_c) := P_N(z_c)\, D_z\mathcal{F}_{\text{int}}(z_c)\big|_{N_{z_c}\mathcal{C}}, \qquad C(z_c,\Gamma) := P_N(z_c)\, D_z\mathcal{F}_{\text{cpl}}(z_c,\Gamma)\Big|_{N_{z_c}\mathcal{C}}.$$

Then the projected Jacobian splits as

$$J_\perp(z_c,\Gamma) = D(z_c) - C(z_c,\Gamma). \tag{7}$$

Assumption: scalar effective-gain specialization. For the threshold theorem below we adopt the following structural specialization on W: there exists a scalar *net effective gain* $g_{\text{eff}}(\Gamma)$ and a C^1 normalized coupling operator $\widetilde{C}(z_c)$ on the normal space such that

$$C(z_c,\Gamma) = g_{\text{eff}}(\Gamma)\,\widetilde{C}(z_c), \qquad z_c \in \mathcal{C}\cap W. \tag{8}$$

This factorization arises, for example, in symmetric coupling architectures and is assumed to hold on $\mathcal{C}\cap W$ within the admissible regime.

Under (8), the transverse Jacobian becomes

$$J_\perp(z_c,\Gamma) = D(z_c) - g_{\text{eff}}(\Gamma)\,\widetilde{C}(z_c).$$

Remark 2 (Edgewise or heterogeneous gains)**.** *If coupling terms involve heterogeneous gains (edgewise κ_{ij}^{eff} and node susceptibilities χ_i), one may define $g_{\min}(t)$ as a uniform lower bound on stabilizing gain factors along W and replace $g_{\text{eff}}(\Gamma)$ in the threshold statements by $g_{\min}(t)$. Stability arguments then proceed with $g_{\min}$ in place of g_{eff}.*

4.3. Symmetric-Part Curvature Bounds in the Fast Subsystem (Normal Space)

We analyze transverse contraction for the fast subsystem obtained by freezing the slow variables ($\varepsilon = 0$), with λ_i acting as parameters on the contraction timescale.

Symmetric parts on the normal subspace. For each $z_c \in \mathcal{C}\cap W$, define the symmetric parts (as operators on $N_{z_c}\mathcal{C}$)

$$D_s(z_c) := \frac{D(z_c)+D(z_c)^\top}{2}, \qquad \widetilde{C}_s(z_c) := \frac{\widetilde{C}(z_c)+\widetilde{C}(z_c)^\top}{2}, \qquad G_s(z_c) := \frac{G(z_c)+G(z_c)^\top}{2}.$$

Uniform normal curvature bounds. Since $\mathcal{C}\cap W$ is compact and all maps are continuous, define

$$\Lambda_D := \sup_{z_c\in\mathcal{C}\cap W}\ \sup_{\substack{v\in N_{z_c}\mathcal{C}\\ \|v\|=1}} v^\top\big(D_s(z_c)+G_s(z_c)\big)v,$$

and

$$\Lambda_C := \inf_{z_c\in\mathcal{C}\cap W}\ \inf_{\substack{v\in N_{z_c}\mathcal{C}\\ \|v\|=1}} v^\top\widetilde{C}_s(z_c)v.$$

The quantity Λ_D bounds the maximal destabilizing normal curvature arising from intrinsic dynamics together with geometric frame variation along $\mathcal{C}$; in particular, the contribution of the geometry operator $G(z_c)$ is absorbed through its symmetric part.

Alignment potential condition. We assume the coupling operator provides uniform positive curvature in the normal direction,

$$\Lambda_C > 0. \tag{9}$$

Condition (9) states that the coupling-induced normal curvature is uniformly positive in symmetric part along $\mathcal{C} \cap \mathcal{W}$.

4.4. Explicit Curvature Dominance and Uniform Normal Contraction

We continue in the fast subsystem ($\varepsilon = 0$) and use the normal variational dynamics (5).

Related contraction-type criteria appear in nonlinear systems analysis, where uniform negativity of the symmetric part of the Jacobian implies exponential convergence of trajectories [12]. Here the contraction strength is modulated by the compatibility-dependent gain $g_{\text{eff}}(\Gamma)$, so that internal compatibility enters directly into the stabilization threshold.

Critical gain level. Define the critical effective gain

$$g_{\text{crit}} := \frac{\Lambda_D}{\Lambda_C}. \tag{10}$$

Lemma 2 (Normal curvature dominance inequality)**.** *Assume* (9)*. Suppose there exists $\mu > 0$ such that*

$$g_{\text{eff}}(\Gamma) \geq g_{\text{crit}} + \mu. \tag{11}$$

Then for all $z_c \in \mathcal{C} \cap \mathcal{W}$ and all unit $v \in N_{z_c}\mathcal{C}$,

$$v^\top \Big(D_s(z_c) + G_s(z_c) - g_{\text{eff}}(\Gamma)\, \widetilde{C}_s(z_c) \Big)\, v < 0.$$

Proof. Fix $z_c \in \mathcal{C} \cap \mathcal{W}$ and $\|v\| = 1$ with $v \in N_{z_c}\mathcal{C}$. By definition of Λ_D and Λ_C,

$$v^\top \big(D_s(z_c) + G_s(z_c) \big) v \leq \Lambda_D, \qquad v^\top \widetilde{C}_s(z_c) v \geq \Lambda_C.$$

Thus

$$v^\top \Big(D_s + G_s - g_{\text{eff}}\, \widetilde{C}_s \Big)\, v \leq \Lambda_D - g_{\text{eff}}\, \Lambda_C,$$

which is negative whenever (11) holds. □

Theorem 1 (Uniform normal contraction toward $\mathcal{C}$ in the fast subsystem)**.** *Assume* (9) *and* (11)*. Then there exist $\delta > 0$ and a neighborhood $U_1 \subset U_0$ of $\mathcal{C} \cap \mathcal{W}$ such that any trajectory of the fast subsystem with initial condition $z(0) \in U_1$ remains in U_1 for all forward time for which the solution exists, and the normal displacement $\eta(t)$ satisfies*

$$\frac{d}{dt} \|\eta(t)\|^2 \leq -2\delta\, \|\eta(t)\|^2 \tag{12}$$

whenever $\|\eta(t)\|$ is sufficiently small. Consequently, $\mathcal{C} \cap \mathcal{W}$ is locally uniformly exponentially attracting in the normal directions for the fast subsystem within the neighborhood U_1.

Proof. Under (11), Lemma 2 implies that the symmetric part of the linear normal operator

$$J_\perp(z_c, \Gamma) + G(z_c) = D(z_c) + G(z_c) - g_{\text{eff}}(\Gamma) \widetilde{C}(z_c)$$

is uniformly negative definite on $\mathcal{C} \cap \mathcal{W}$ when restricted to $N_{z_c}\mathcal{C}$.

Because $g_{\text{eff}}(\Gamma) \geq g_{\text{crit}} + \mu$ and $\Lambda_C > 0$, Lemma 2 yields a uniform negative bound with margin $\mu\Lambda_C$. Hence, with

$$\delta := \mu \Lambda_C > 0,$$

we have for all $z_c \in \mathcal{C} \cap \mathcal{W}$ and all $v \in N_{z_c}\mathcal{C}$,

$$v^\top \big(D_s(z_c) + G_s(z_c) - g_{\text{eff}}(\Gamma) \widetilde{C}_s(z_c) \big) v \leq -\delta \|v\|^2.$$

Using the normal variational form (5),

$$\frac{d}{dt} \|\eta\|^2 = 2\eta^\top \big(J_\perp(z_c, \Gamma) + G(z_c) \big) \eta + \mathcal{O}(\|\eta\|^3) \leq -2\delta \|\eta\|^2 + \mathcal{O}(\|\eta\|^3).$$

Shrinking U_1 if necessary ensures that the cubic remainder is dominated by the quadratic term, yielding (12). □

Relation to classical threshold behavior. Theorem 1 shows that the present framework recovers a classical threshold mechanism in geometric form: stability is obtained once a stabilizing interaction term dominates the intrinsic transverse destabilization. The novelty is that the relevant gain is not externally tuned, but arises endogenously through the compatibility–integration cascade.

4.5. Local Contraction of the Mismatch Observable

We now translate normal contraction toward $\mathcal{C}$ into contraction of the mismatch observable $e(t) = E(z(t))$.

Critical threshold. Let g_{crit} be the critical gain defined in (10). Whenever $g_{\mathrm{eff}}(\Gamma) \geq g_{\mathrm{crit}} + \mu$ for some $\mu > 0$, Theorem 1 implies local exponential decay of $\mathrm{dist}(z(t), \mathcal{C}) = \|\eta(t)\|$.

Corollary 1 (Exponential decay of mismatch under normal contraction)**.** *Under the hypotheses of Theorem 1, there exist constants $c_1, c_2, \delta > 0$ and a neighborhood U_1 of $\mathcal{C} \cap \mathcal{W}$ such that for any trajectory $z(t) \in U_1$,*

$$\|E(z(t))\| \leq c_1 e^{-\delta t} \|E(z(0))\|, \tag{13}$$

and equivalently

$$\|E(z(t))\| \leq c_2 e^{-\delta t} \,\mathrm{dist}(z(0), \mathcal{C}).$$

Proof. By Lemma 1, there exist constants $m, M > 0$ such that for all z in a neighborhood U_1 of $\mathcal{C} \cap \mathcal{W}$,

$$m\|\eta(z)\| \leq \|E(z)\| \leq M\|\eta(z)\|.$$

By Theorem 1, the transverse deviation satisfies

$$\|\eta(t)\| \leq c\, e^{-\delta t} \|\eta(0)\|$$

for some constant $c > 0$ and for trajectories remaining in U_1.

Combining these bounds yields

$$\|E(z(t))\| \leq M\|\eta(t)\| \leq Mc\, e^{-\delta t} \|\eta(0)\| \leq \frac{Mc}{m}\, e^{-\delta t} \|E(z(0))\|.$$

Renaming constants yields the exponential decay bound (13). □

Interpretation. The stabilization mechanism is geometric. Once the net effective gain $g_{\mathrm{eff}}(\Gamma)$ exceeds the threshold g_{crit}, the fast subsystem becomes locally contractive toward the compatibility manifold in the normal directions. The observable mismatch $E(z)$ therefore decays exponentially as a consequence of distance-to-manifold contraction, rather than serving as the fundamental transverse coordinate. This recovers, in geometric form, a standard threshold phenomenon of nonlinear dynamics: once interaction strength crosses a critical level, coherent behavior becomes locally stable.

4.6. Structural Consequences of the Modulation Architecture

We collect several structural consequences of the factorized integration–susceptibility modulation architecture introduced in Section 3. In this architecture the pairwise effective coupling coefficients take the multiplicatively separable form

$$\kappa_{ij}^{\mathrm{eff}}(\Gamma_i, \Gamma_j) = \kappa_{ij}\, Q(\Gamma_i) R(\Gamma_j),$$

so that the interaction strength between subsystems is modulated by their respective integration levels.

The statements below are independent of the curvature-dominance condition derived in Subsection 4.4 and follow directly from the definitions in Section 3.

Monotonicity of effective coupling.

Proposition 1 (Integration–coupling monotonicity)**.** *Let $\kappa_{ij} \geq 0$ and assume $Q, R \in C^1(\mathbb{R}_{\geq 0})$ are non-negative and non-decreasing. Then*

$$\kappa_{ij}^{\mathrm{eff}}(\Gamma_i, \Gamma_j) = \kappa_{ij}\, Q(\Gamma_i) R(\Gamma_j)$$

is non-decreasing in each argument.

Proof. Since $\kappa_{ij} \geq 0$, $Q(\Gamma_i) \geq 0$, and $R(\Gamma_j) \geq 0$, we have

$$\partial_{\Gamma_i} \kappa_{ij}^{\text{eff}} = \kappa_{ij} Q'(\Gamma_i) R(\Gamma_j) \geq 0, \qquad \partial_{\Gamma_j} \kappa_{ij}^{\text{eff}} = \kappa_{ij} Q(\Gamma_i) R'(\Gamma_j) \geq 0.$$

Thus κ_{ij}^{eff} is non-decreasing in each argument. □

Incompatibility ordering.

Proposition 2 (Incompatibility–integration ordering)**.** *Assume $A'(F) < 0$, $\Xi'(\alpha) > 0$, and $T'(\alpha) > 0$. Then $\Gamma_i(F_i)$ is non-increasing as a function of F_i. Consequently, reduction of incompatibility induces non-decreasing effective coupling strength.*

Proof. Reduction of F_i increases $\alpha_i = A(F_i)$. Since $\Xi'(\alpha) > 0$ and $T'(\alpha) > 0$, both ξ_i and τ_i increase, hence $\Gamma_i = \xi_i \tau_i$ increases. Monotonicity of κ_{ij}^{eff} then follows from Proposition 1. □

Susceptibility amplification.

Proposition 3 (Bounded susceptibility amplification)**.** *Assume $\rho_i \leq C_{\text{dest}}$ on W and $S'(\mu) \leq 0$. Then $\chi_i = S(\rho_i)$ is bounded on W. Moreover, any decrease of ρ_i induces a non-decreasing susceptibility.*

Proof. Since W is compact and ρ_i is continuous on W, there exists $\rho_{\max} \leq C_{\text{dest}}$ such that $\rho_i(W) \subset (-\infty, \rho_{\max}]$. Continuity of S implies $\chi_i = S(\rho_i)$ is bounded on W. If ρ_i decreases and $S' \leq 0$, then $S(\rho_i)$ is non-decreasing. □

Strict subfamily property.

Proposition 4 (Strict subfamily of state-dependent couplings)**.** *The factorized class*

$$\kappa_{ij}^{\text{eff}} = \kappa_{ij} Q(\Gamma_i) R(\Gamma_j)$$

is a strict subset of generic C^1 state-dependent coupling laws.

Proof. A generic state-dependent coupling may depend arbitrarily on (Γ_i, Γ_j). In contrast, the factorized class restricts the dependence to a multiplicatively separable form. Generic bivariate functions are not multiplicatively separable; for example, a function such as $g(\Gamma_i + \Gamma_j)$ cannot, in general, be represented as $Q(\Gamma_i) R(\Gamma_j)$. Hence the factorized class is a strict subset.

This restriction also has structural consequences for the present framework. The multiplicatively factorized form allows each node's integration scale to modulate interactions through separate sender and receiver gain factors while preserving the baseline interaction topology. As a result, effective coupling strength can increase monotonically without introducing new interaction channels. □

Classical limit.

Proposition 5 (Classical coupling limit)**.** *If $Q \equiv 1$, $R \equiv 1$, and $\chi_i \equiv 1$, then $\kappa_{ij}^{\text{eff}} = \kappa_{ij}$ and the system reduces to a classical fixed-coupling architecture.*

Proof. Immediate from substitution. □

4.7. Integration-Dependent Synchronization in Networked Oscillators

We consider a connected undirected graph $\mathcal{G} = (\mathcal{V}, \mathcal{E})$ with N nodes and Laplacian matrix L.

Let $\nu_2 > 0$ denote the second-smallest eigenvalue of the Laplacian L (the algebraic connectivity).

Each node evolves according to

$$\dot{x}_i = f_i(x_i) - \sum_{j=1}^{N} \kappa_{ij}^{\text{eff}} a_{ij} H(x_i - x_j),$$

where

- a_{ij} are adjacency weights,
- H is C^1 with $H(0) = 0$,
- $\kappa_{ij}^{\text{eff}} = \kappa_{ij} Q(\Gamma_i) R(\Gamma_j)$,
- $\kappa_{ij} \geq 0$ are baseline couplings.

Synchronization manifold (identical case). Assume $f_i \equiv f$ for all i. Then the synchronization manifold

$$\mathcal{S} = \{x_1 = x_2 = \cdots = x_N\}$$

is invariant.

Let $s(t)$ denote the synchronized trajectory satisfying $\dot{s} = f(s)$.

This setting provides a direct connection to classical synchronization theory: the resulting threshold condition recovers the familiar competition between intrinsic divergence, coupling strength, and network connectivity, but with effective coupling now generated endogenously through the integration variables.

Linearization transverse to $\mathcal{S}$. Linearizing about $\mathcal{S}$ yields transverse dynamics

$$\dot{\xi} = \left[I_N \otimes Df(s) - \kappa_{\text{eff}}\, L \otimes DH(0)\right] \xi, \qquad \kappa_{\text{eff}} := \kappa_{\min}\, Q(\Gamma_{\min}) R(\Gamma_{\min}).$$

Theorem 2 (Integration-dependent synchronization threshold)**.** *Assume:*

1. *Df is continuous and bounded on W, and there exists $C_{\text{dest}} \geq 0$ such that*

$$\sup_{x \in W} \sup_{\lambda \in \sigma(Df(x))} \text{Re}(\lambda) \leq C_{\text{dest}};$$

2. *$DH(0)$ is positive definite in the coupling direction, with minimal eigenvalue $\beta > 0$;*
3. *the graph is connected ($\nu_2 > 0$).*

Let

$$\Gamma_{\min} := \min_i \Gamma_i.$$

If

$$\kappa_{\min} Q(\Gamma_{\min}) R(\Gamma_{\min}) \nu_2 \beta > C_{\text{dest}},$$

then the synchronization manifold $\mathcal{S}$ is locally exponentially attracting for trajectories that remain in the admissible regime W.

Proof. Decomposition into Laplacian eigenmodes yields transverse blocks of the form

$$Df(s) - \kappa_{\text{eff}} \nu_k DH(0), \qquad k \geq 2.$$

By definition,

$$\kappa_{\text{eff}} = \kappa_{\min} Q(\Gamma_{\min}) R(\Gamma_{\min}),$$

the worst case corresponds to ν_2. If the real part of all transverse eigenvalues is strictly negative, uniform exponential contraction follows. □

Relation to classical synchronization conditions. Theorem 2 recovers the standard form of a network synchronization threshold, in which stability is governed by the competition between intrinsic node-level divergence and Laplacian-weighted coupling strength. Here, however, the effective gain is not prescribed externally, but is modulated through the compatibility–integration cascade.

4.8. Unified Threshold Structure Across Scales

The stabilization mechanisms established in Theorem 1 and Theorem 2 share a common structural form.

In both cases, transverse stability is determined by a competition between intrinsic destabilizing curvature or divergence and integration-modulated stabilizing interaction strength. The common dominance structure governing these mechanisms is illustrated schematically in Fig. 3.

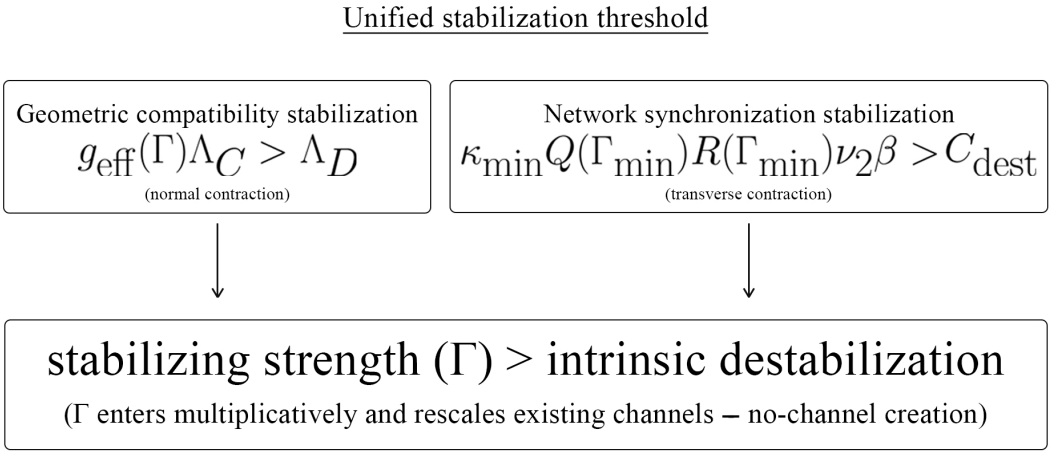

Figure 3: Unified stabilization threshold. Left: geometric compatibility stabilization governed by $g_{\mathrm{eff}}(\Gamma)\Lambda_C > \Lambda_D$. Right: network synchronization stabilization governed by $\kappa_{\min} Q(\Gamma_{\min}) R(\Gamma_{\min}) \nu_2 \beta > C_{\mathrm{dest}}$. In both cases stability arises when integration-modulated stabilizing strength exceeds intrinsic destabilization.

The schematic comparison in Fig. 3 highlights that both geometric compatibility stabilization and network synchronization follow the same dominance principle: stabilization occurs when integration-modulated interaction strength exceeds intrinsic destabilizing curvature or divergence.

Taken together, these results show that the present framework does not merely introduce a new coupling architecture; it recovers a common threshold structure already familiar from classical nonlinear dynamics and synchronization theory, while explaining how such thresholds may be crossed through endogenous modulation of effective coupling.

In the geometric compatibility setting (Subsection 4.4), stability is achieved when the effective coupling dominates the maximal transverse curvature.

In the network synchronization setting (Subsection 4.7), stability is achieved when

$$\kappa_{\min} Q(\Gamma_{\min}) R(\Gamma_{\min}) \nu_2 \beta > C_{\mathrm{dest}},$$

so that Laplacian-weighted interaction strength dominates intrinsic divergence.

Synchronization stability in coupled oscillator networks is commonly studied using the Master Stability Function framework introduced by Pecora and Carroll [13] and extended to complex network structures in [2, 1]. The compatibility-based formulation developed here can be viewed as a geometric extension in which stability thresholds depend on integration-modulated interaction strength rather than fixed coupling parameters alone.

In both cases, the integration scale Γ enters multiplicatively into the effective gain. Higher integration therefore lowers the baseline coupling required for stabilization without altering the underlying structural connectivity (curvature geometry or graph topology).

This reveals a scale-consistent dominance principle: integration does not introduce new interaction channels, but rescales the effective strength of existing ones. Stabilization occurs when integration-modulated interaction strength exceeds the intrinsic destabilizing curvature or divergence of the system.

5. Discussion

The integration-modulated coupling structure yields several structural consequences within classical nonlinear dynamical systems theory and provides a mechanism through which familiar threshold-governed behaviors can arise from endogenous modulation of interaction strength.

First, effective coupling becomes internally generated: its amplitude is determined by derived integration variables rather than externally prescribed parameters. Under monotone incompatibility decay, the integration scale is non-decreasing along admissible trajectories and may drive effective coupling across finite stabilization thresholds while preserving the baseline interaction topology. Threshold activation therefore arises from internal modulation rather than the introduction of new interaction channels, providing a structural explanation for how systems may cross classical stability thresholds without external parameter tuning.

Second, compatibility states become conditionally attracting once the effective coupling exceeds a transverse spectral threshold. Within the admissible regime W, distance to the compatibility manifold contracts exponentially in the fast subsystem, yielding exponential decay of cross-system mismatch and recovering the standard dynamical signature of threshold-induced stabilization.

Third, the structure suggests a natural hierarchical extension in which similar compatibility cascades may arise across multiple scales of interacting subsystems. The present analysis, however, remains at the level of local contraction and threshold-triggered alignment.

Fourth, susceptibility modulation interacts multiplicatively with the integration-mediated coupling within the admissible regime. Provided the standing spectral and boundedness assumptions hold on W, this modulation alters interaction strength but does not change the baseline interaction graph.

The results rely solely on the regularity, monotonicity, spectral-bound, and contraction assumptions specified in Section 3.12. No additional dynamical principles are introduced; the stabilization mechanism follows directly from the curvature-dominance inequalities and local contraction toward the compatibility manifold within the admissible regime. Taken together with the results of Section 4, this shows that the compatibility–integration cascade does not introduce a new class of stability conditions, but instead provides a structural mechanism that reproduces known threshold phenomena within a constrained endogenous coupling architecture.

Structural role of the compatibility cascade. Taken together, the results of this paper show that the incompatibility–integration cascade provides a structural mechanism linking internal geometric alignment to increased interaction strength. Reduction of local incompatibility relative to the compatibility manifold increases the integration scales Γ_i, which in turn modulate the effective couplings $\kappa_{ij}^{\mathrm{eff}}$ through the factorized interaction law. Once these effective couplings exceed the intrinsic destabilizing curvature bounds, the system enters a regime in which transverse contraction or synchronization becomes possible. In this way the cascade provides a mechanism through which progressive internal coherence within subsystems accumulates into stronger dynamical coupling and ultimately into collective stabilization.

Robustness considerations. The stabilization mechanism described here is structural and depends only on the curvature-dominance inequalities and boundedness assumptions specified on the admissible regime W. Perturbations of the vector field or slow variables that preserve these bounds do not alter the threshold structure, indicating that the mechanism is structurally stable within the admissible regime; a detailed robustness analysis lies outside the scope of the present work.

6. Scope and Structural Boundaries

The results of Sections 3–4 hold under the regularity, spectral-bound, monotonicity, and admissibility assumptions specified in Section 3.12. In particular, forward invariance of the admissible regime, boundedness on W, and the fast-subsystem reduction obtained by freezing the slow variables ($\varepsilon = 0$) justify the local contraction analysis carried out in Section 4.

The incompatibility functional F_i is defined abstractly but must be continuously differentiable and compatible with the ordered monotone cascade

$$F_i \longmapsto \alpha_i \longmapsto (\xi_i, \tau_i) \longmapsto \Gamma_i \longmapsto \kappa_{ij}^{\mathrm{eff}}.$$

The framework constrains monotonicity and factorized modulation along this chain but does not prescribe specific parametric forms for the constituent maps.

Composite stabilization is conditional. Contraction toward the compatibility manifold requires:

- monotone incompatibility decay within a forward-invariant regime,
- effective coupling exceeding a finite transverse spectral threshold,

- persistence of a transverse spectral gap,
- robustness under slow structural drift.

If any of these conditions fail, composite formation need not occur within the present structural class.

The integration scale Γ_i modulates effective coupling exclusively through pre-existing interaction channels. Baseline invariance,

$$\kappa_{ij} = 0 \implies \kappa_{ij}^{\mathrm{eff}} = 0,$$

is preserved throughout.

The analysis is confined to classical nonlinear fast–slow systems. Microscopic derivations of integration-scale dynamics, stochastic destabilization mechanisms beyond bounded perturbations, and extensions outside invariant manifold and contraction theory lie beyond the scope of this work.

These assumptions define the regime of applicability of the proposed structural class.

7. Conclusion

We have introduced and analyzed a constrained class of integration-modulated coupling structures for coupled nonlinear fast–slow systems. Under monotone incompatibility decay and standard regularity, spectral-bound, and timescale-separation assumptions, effective coupling increases endogenously through a derived integration scale. When a finite transverse threshold is exceeded within the admissible regime, distance to the compatibility manifold contracts locally and trajectories converge exponentially toward compatibility states, thereby recovering a standard threshold mechanism of nonlinear dynamics through endogenous modulation of interaction strength.

The compatibility–integration cascade can be iterated on composite observables in regimes where stabilization yields sustained proximity to compatibility. This suggests a hierarchical extension of the same threshold mechanism across multiple levels of interacting subsystems, without altering the baseline interaction topology, while the present results remain at the level of threshold-triggered local contraction toward compatibility states.

All results are obtained entirely within classical nonlinear dynamical systems theory. Stabilization arises through constrained modulation of pre-existing coupling channels, without introduction of additional interactions, showing that the mechanism operates within standard dynamical frameworks rather than requiring new dynamical principles.

The contribution is structural: identification of a minimal monotone cascade linking incompatibility decay, integration growth, and threshold-driven stabilization, which provides a unifying mechanism underlying threshold phenomena across geometric contraction and network synchronization settings.

Declaration of Generative AI in Scientific Writing

During the preparation of this manuscript, generative AI tools were used to assist with drafting, language editing, and structural development of the text. The author reviewed, edited, and takes full responsibility for the final content of the manuscript.

References

[1] Arenas, A., Díaz-Guilera, A., Kurths, J., Moreno, Y., Zhou, C., 2008. Synchronization in complex networks. Physics Reports 469, 93–153. doi:10.1016/j.physrep.2008.09.002.

[2] Barahona, M., Pecora, L.M., 2002. Synchronization in small-world systems. Physical Review Letters 89, 054101. doi:10.1103/PhysRevLett.89.054101.

[3] Fenichel, N., 1971. Persistence and smoothness of invariant manifolds for flows. Indiana University Mathematics Journal 21, 193–226.

[4] Fenichel, N., 1979a. Geometric singular perturbation theory for ordinary differential equations. Journal of Differential Equations 31, 53–98.

[5] Fenichel, N., 1979b. Geometric singular perturbation theory for ordinary differential equations. Journal of Differential Equations 31, 53–98.

[6] Guckenheimer, J., Holmes, P., 1983. Nonlinear Oscillations, Dynamical Systems, and Bifurcations of Vector Fields. Springer, New York.

[7] Hirsch, M.W., Pugh, C.C., Shub, M., 1977a. Invariant Manifolds. Springer, Berlin.

[8] Hirsch, M.W., Pugh, C.C., Shub, M., 1977b. Invariant Manifolds. Springer, Berlin.

[9] Jones, C.K.R.T., 1995. Geometric singular perturbation theory, in: Dynamical Systems (Montecatini Terme, 1994). Springer, Berlin. volume 1609 of *Lecture Notes in Mathematics*, pp. 44–118.

[10] Kuehn, C., 2015. Multiple Time Scale Dynamics. Springer, Cham.

[11] Kuramoto, Y., 1984. Chemical Oscillations, Waves, and Turbulence. Springer, Berlin.

[12] Lohmiller, W., Slotine, J.J.E., 1998. On contraction analysis for nonlinear systems. Automatica 34, 683–696. doi:10.1016/S0005-1098(98)00019-3.
[13] Pecora, L.M., Carroll, T.L., 1998. Master stability functions for synchronized coupled systems. Physical Review Letters 80, 2109–2112.
[14] Pikovsky, A., Rosenblum, M., Kurths, J., 2001. Synchronization: A Universal Concept in Nonlinear Sciences. Cambridge University Press, Cambridge.
[15] Strogatz, S.H., 2015. Nonlinear Dynamics and Chaos. 2 ed., Westview Press, Boulder.
[16] Wiggins, S., 1994. Normally Hyperbolic Invariant Manifolds in Dynamical Systems. Springer, New York.

Appendix

Symmetric specialization for the oscillator reduction. To exhibit the threshold mechanism in a classical setting, we consider a symmetric specialization of the general coupling architecture in which $\kappa_{12}^{\mathrm{eff}} = \kappa_{21}^{\mathrm{eff}} =: \kappa^{\mathrm{eff}}$. This corresponds to identical gain modulation for the interacting nodes and allows the mismatch dynamics to be written in a single scalar form. The following section presents a minimal oscillator reduction of the general mechanism.

A. Phase Oscillators with Integration–Modulated Coupling

Consider two phase oscillators

$$\dot{\theta}_1 = \omega_1 + \kappa_{21}^{\mathrm{eff}} \sin(\theta_2 - \theta_1), \qquad \dot{\theta}_2 = \omega_2 - \kappa_{12}^{\mathrm{eff}} \sin(\theta_2 - \theta_1),$$

with baseline coupling coefficients $\kappa_{ij} \geq 0$.

Define the phase mismatch

$$e := \theta_2 - \theta_1, \qquad \Delta\omega := \omega_2 - \omega_1.$$

For symmetric baseline coupling $\kappa_{12} = \kappa_{21} = \kappa$, the effective coupling has the factorized form

$$\kappa^{\mathrm{eff}} = \kappa\, Q(\Gamma_1) R(\Gamma_2).$$

This provides a concrete instantiation of the threshold mechanism derived in Section 4 within a classical phase oscillator model, showing how the general curvature-dominance condition reduces to a classical phase-locking threshold under integration-modulated coupling.

The reduced mismatch dynamics are

$$\dot{e} = \Delta\omega - \kappa^{\mathrm{eff}} \sin e.$$

A phase-locked solution e^* exists if and only if

$$|\Delta\omega| < \kappa^{\mathrm{eff}}.$$

Linearization at e^* yields

$$\frac{d}{dt}(\delta e) = -\kappa^{\mathrm{eff}} \cos(e^*)\, \delta e.$$

If $\cos(e^*) > 0$, the locked solution is locally exponentially stable.

Non-decreasing integration scales Γ_i increase κ^{eff} and therefore enlarge the classical detuning interval admitting stable phase-locking.

Illustration of cascade-driven threshold crossing. Within the structural framework of the present paper, the effective coupling $\kappa^{\mathrm{eff}} = \kappa Q(\Gamma_1) R(\Gamma_2)$ is modulated by the integration scales Γ_i. If the incompatibility functionals F_i decrease along trajectories, the cascade

$$F_i \longmapsto \alpha_i \longmapsto (\xi_i, \tau_i) \longmapsto \Gamma_i$$

implies that Γ_i are non-decreasing. Consequently κ^{eff} may increase during system evolution, allowing the oscillator pair to cross the classical locking threshold $|\Delta\omega| < \kappa^{\mathrm{eff}}$. This shows that the compatibility–integration cascade can drive a system from a drifting regime into a phase-locked regime without modifying the baseline coupling coefficient κ, thereby recovering a classical locking transition through purely endogenous modulation of effective coupling strength.